

AN EXPERIMENTAL INVESTIGATION OF HELICOPTER SLIPSTREAM IN THE PRESENCE OF ELEVATED HELIPORT

Paweł Ruchala, pawel.ruchala@ilot.edu.pl, Łukasiewicz Research Network – Institute of Aviation (Poland)

Wit Stryczniewicz, wit.stryczniewicz@ilot.edu.pl, Łukasiewicz Research Network – Institute of Aviation (Poland)

Adam Dziubiński, adam.dziubinski@ilot.edu.pl, Łukasiewicz Research Network – Institute of Aviation (Poland)

Romana Ratkiewicz, roma@cbk.waw.pl, Space Research Centre (Poland)

Abstract

An unsteadiness of pressure in a helicopter rotor slipstream may bring a significant problem during operation from the elevated heliports, as the oscillating slipstream acts on the heliport plate and causes vibration of building's structure. However, still it is an unappreciated issue, discussed mainly in the literature focused on the brownout. In this case researchers usually neglect the loads acting on the ground. On the other hand, investigations of interaction between rotor slipstream and helicopter's surroundings, e.g. [7], [4], are often limited to a time-averaged case. Meanwhile, results of the investigation presented in the paper show that amplitude of the pressure oscillation cannot be omitted, as it can achieve its value of roughly 50% of the rotor disc load. This value, however, is dependent on thrust coefficient and height above the ground. Presented results have been obtained in an experimental way, using the helicopter with the rotor diameter of 0.7 m and validated by comparison with the full-scale rotor (with its diameter of 8 m).

1. INTRODUCTION

1.1. The use of elevated heliports

An elevated heliport, as it has been defined by FAA (Federal Aviation Administration), is a heliport located on a rooftop or other elevated structure where the TLOF (touchdown and liftoff area) is at least 30 inches (76 cm) above the surrounding surface [6]. Elevated heliports are commonly used in densely populated areas (e.g. cities), especially for life saving. In this case, the time needed to transport a patient to a hospital must be minimized at all costs – but with respective safety. Consequences of this fact may be observed e.g. in evidence of airports and heliports, by Polish Civil Aviation Authority (Urząd Lotnictwa Cywilnego) [18]. Until February, 2019 this evidence covered 40 elevated heliports in Poland, including 35 medical heliports and only 5 general purpose ones. Thus elevated heliports make up to

18% of 198 medical heliports in Poland and 14% of all 276 ones. It also must be noted that first elevated heliport in this evidence has been included quite recently – in 2011 [12].

It is worth to analyze reasons of the fact that a vast majority of all heliports (both elevated and located on the ground level) are medical ones. In case of life saving, a reduction of total travel time is much more important, than disadvantages of the helicopter transport, e.g. operational costs, noise and safety. Abovementioned issues terminated the concepts of “common helicopter transport”; it must be noted that shortly after World War 2 the helicopter, which became an usable mean of transport, to many observers seemed to promise the wings for city dwellers, who might land atop their apartments or office buildings [3]. A nail in the coffin for these ideas was an accident during landing on the heliport atop of the Pan Am Building in New York in May, 1977. A failure of the landing gear of Sikorsky S-61L helicopter caused its collapse, due to which the rotor blades felt off. As it was described in the New York Times article, whirling like a gigantic boomerang the blade struck four people on the rooftop land pad, killing three instantly, then plunged over the skyscraper's west parapet. (...) One piece of blade continued to fall, whirling onto Madison Avenue and killing a woman walking on Madison and 43rd Street shortly after 5.30pm [1]. As a result, a development of heliports in densely populated areas (e.g. cities)

Copyright Statement

The authors confirm that they, and/or their company or organization, hold copyright on all of the original material included in this paper. The authors also confirm that they have obtained permission, from the copyright holder of any third party material included in this paper, to publish it as part of their paper. The authors confirm that they give permission, or have obtained permission from the copyright holder of this paper, for the publication and distribution of this paper as part of the ERF proceedings or as individual offprints from the proceedings and for inclusion in a freely accessible web-based repository.

has been limited for many years, and air operations from elevated heliports are, in vast majority, related only with emergency cases.

1.2. Aerodynamic issues related with elevated heliports

Designing of an elevated heliport is relatively complex, as it cannot be treated as a standalone add-on to a project. In fact, it is very closely interlinked – sometimes in surprising ways – with rest of the project [16]. One of these connections, which must be taken into account by the architects designing a heliport, is the aerodynamic interaction between the helicopter and a building with the heliport on its top. One of the simplest and most commonly referred examples of this interaction is the rotor slipstream in the ground effect (IGE). In its structure one can distinguish four regions [14], as it has been presented in Figure 1:

1. Contraction, where the slipstream velocity is directed more or less vertically – similar to the OGE (out of ground effect) case;
2. Transition, where interaction with the ground turns the flow to the horizontal direction along the ground
3. Outwash, where the flow is directed along the ground and its peak value decays with increase in radial distance
4. Recirculation, where the flow is induced by the slipstream due to air viscosity

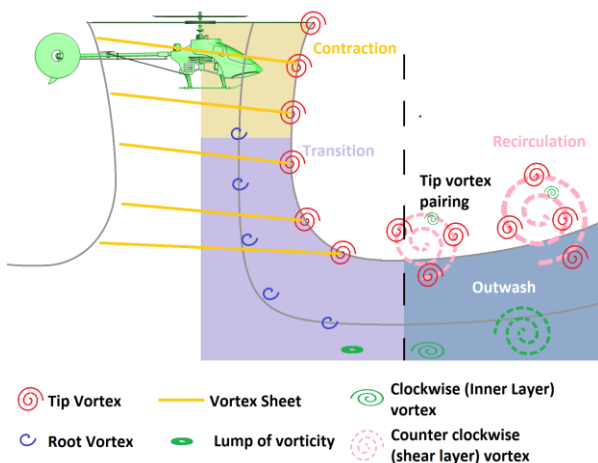


Figure 1. The slipstream of a helicopter rotor in the ground effect (based on [14])

The picture of the slipstream presented above assumes that the ground is a flat, infinitely large surface. In reality, especially in case of elevated heliports, such assumption cannot be made.

Aerodynamic interaction between the rotor slipstream and obstacles in its surroundings is a quite important research subject and several numerical and experimental studies have been published in the scientific literature [7]. Recently this topic was thoroughly investigated e.g. within GARTEUR Action Group HC/AG-22 project which deals with the basic research about the forces acting on obstacles when immersed in rotor wakes [17]. Safety of helicopter operations on heliports was also investigated in reference to specific heliports, e.g. in USA [8] and in Poland – especially in Institute of Aviation, as a part of activities devoted to improvement of helicopter operation safety [4], [10], [5]. However, these activities were focused mostly on the impact of the building (with its surroundings) on the helicopter performance and stability. Meanwhile, the reversed interaction should not be neglected. A commonly cited example is a hover above the elevated heliport and surrounding buildings (Figure 2, [4]). The slipstream of the helicopter rotor has a tendency for descending down if the nearest roof is lower than the helipad surface, especially when the roof is pitched. It may cause additional wind loads acting on buildings nearby the heliport, which should be taken into account to avoid damage of already existing buildings – especially their cladding. The deflected slipstream may also have its impact on the wind comfort of pedestrians and damage loose objects on the sidewalks.

The phenomena described above assumed that the rotor slipstream is steady, which is a common simplification. In fact, rotor flow is inherently unsteady because of the presence of a finite number of blades. Lifting blades are producing the tip vortices, root vortices, vortex sheets, and oscillations in the inflow (from blade passage). The interaction among these features, as the flow develops, makes the flow field fundamentally unsteady [14]. Moreover, the flow becomes aperiodic because of the self- and mutually induced effects of the strong blade tip vortices [2].

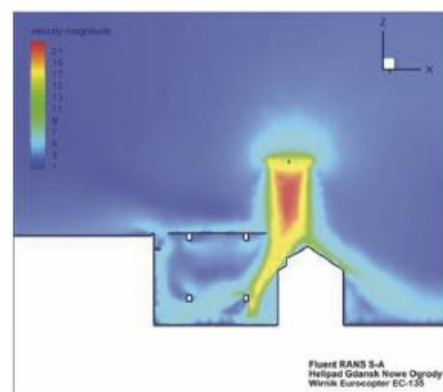


Figure 2. Slipstream velocity magnitude during a hover above a building nearby an elevated heliport^[4]

The unsteadiness of slipstream itself becomes even more significant in proximity of ground. In this case the tip vortices, which flow helically from blade tips, tend to join together and grow in the outwash area due to friction. Secondly, in the boundary layer of the ground, in the outwash zone, a flow separation bubble may also appear. Separation bubbles are created when the static pressure reaches a minimum directly underneath the vortex flow, and then the developing boundary layer faces a steep adverse pressure gradient downstream of the vortex as a consequence of the slower moving fluid and higher pressures there. This pressure gradient can become strong enough to produce localized flow separation and to form a separation bubble^[9] as it has been presented in Figure 3.

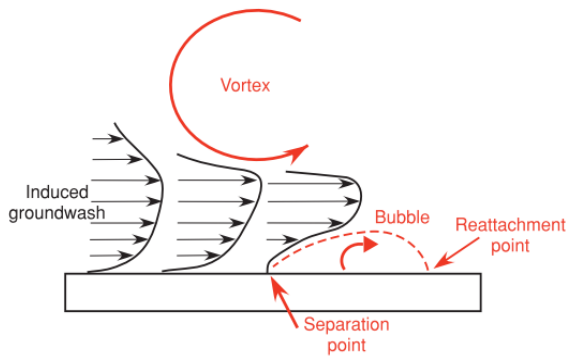


Figure 3. Creation of the separation bubble in the boundary layer of the ground^[9]

The unsteadiness of rotor slipstream may result with vibrations of the heliport, including a structure of the building underneath. In general, a helicopter creates vibration at the landing pad in three ways: (1) turbulence from the rotors, (2) motion from the engine and rotors and (3) impact from the landing itself^[16]. The most important way is the first one, related mostly with helical tip vortices created on the tips of blades. The frequency of these vibrations equals a multiplication of rotor rotation frequency and number of blades^[16] – thus for commonly used (e.g. in Polish Medical Service) Eurocopter EC-135 helicopter, frequency of such vibrations will be about 25 Hz. The frequency of such oscillation is in range of frequencies, which should be analyzed due to its impact on people and buildings (up to 80 Hz^[13]).

Vibrations caused by the rotor slipstream are especially important in case of medical heliports, located close to hospitals. According to PN-B-02171 norm, the allowable acceleration (or velocity) of vibrations in a surgery is even 32

times less, than in case of apartments and 64 times less, than in case of offices^[13]. Taking into account that a major vast of elevated heliports is located in hospitals, one may appreciate an importance of such problem. However, elevated heliports located in non-medical buildings also are the source of the problem: they cause the increased wear of upper part of the building or devices mounted on its roof. In some cases the risk of failure of elevator drives is 45% higher than in a building without heliport^[11].

2. EXPERIMENTAL SETUP

2.1. Test stand

The investigation presented in the paper was aimed on estimation of the unsteady loads acting on the heliport. Within the investigation the remotely controlled helicopter T-REX 450 has been utilized. The rotor diameter of this helicopter was 0.71 m (2.33 ft) and its revolution speed was 2100 RPM. The helicopter rotor was placed above the flat plate, which simulated the heliport's deck (Figure 4). Dimensions of the plate was 1.8 m by 2.1 m; according to Gibertini et al.^[7], the influence of plate's edges for such size (referred to the rotor size) is negligible as the helicopter is located over the center of the plate. The plate was equipped in 11 pressure taps, plugged with flexible tubing to the ESP-32HD-DTC multichannel pressure scanner, connected to the DTC Initium measurement unit. The scanner range was 2450 Pa = 0.36 psi, standard measurement accuracy was 1.5 Pa = 0.0002 psi (0.06%FS) and sampling rate was set to 500 Hz.



Figure 4. The T-REX 450 helicopter over the simulated heliport

To measure rotor thrust and torque, the helicopter was mounted on the 6-component strain gage balance WDP-01. The range and 95% expanded measurement uncertainty of the axial force (thrust) was 30 N and 0.11 N (0.177% of full

scale) respectively. For the torque these values was 7 Nm and 0.06 Nm (0.458% of full scale) respectively.

Additionally, the optical tachometer has been applied to measure the revolution speed of the rotor. The tachometer registered when the rotor blade (only one with a piece of reflective foil) crossed its laser beam, and reacted by generation a TTL impulse. That way the proper rotor RPM was measured, instead a “blade to blade” frequency. These impulses were acquired by a counter channel of the National Instruments USB-6259 universal I/O card. The same card was used to measure loads acting on the strain-gage balance.

The measure equipment was connected to a PC computer with the in-house data acquisition software, created in LabVIEW 2015 environment. The scheme of measurement equipment has been presented in Figure 5.

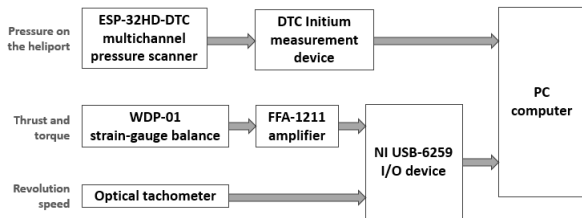


Figure 5. Scheme of measurement equipment

A typical test included several values of collective pitch, set for roughly 10 seconds each. All remaining parameters, including revolution speed and helicopter position versus simulated heliport, were kept constant. Periods of steady conditions have been marked using Boolean marker, written in the data file with other measured parameters. An exemplary process of test has been presented in Figure 6.

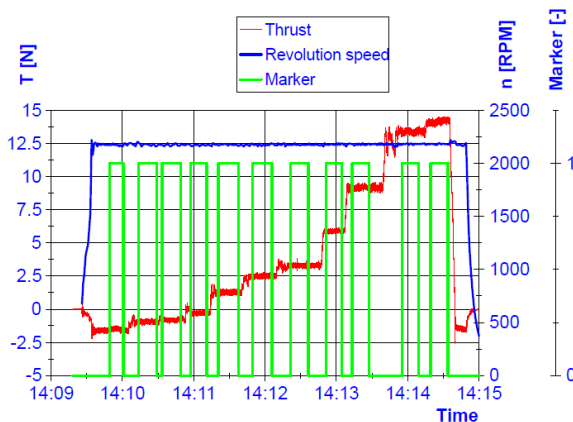


Figure 6. Process of an exemplary test

2.2. Data reduction

The data gathered using measurement equipment described above were collected in TDMS files, separately for the pressures from DTC Initium and for voltages from the NI-6259 card. Using the same computer for data acquisition from both sources ensured that the data were time-synchronized. The data postprocessing included:

- merging data from both sources;
- calculation the loads, including thrust and torque, acting on the strain-gage balance (using its calibration matrix);
- calculation rotor revolution speed, based on the time between successive impulses from the tachometer;
- nondimensionalization of thrust and torque by calculation the thrust coefficient C_T , torque coefficient C_Q and figure of merit FM:

$$(1) \quad C_T = \frac{T}{\rho \cdot A \cdot \omega^2 \cdot R^2}$$

$$(2) \quad C_Q = \frac{Q}{\rho \cdot A \cdot \omega^2 \cdot R^3}$$

$$(3) \quad FM = \frac{C_T^{3/2}}{C_Q \cdot \sqrt{2}}$$

where:

T – rotor thrust

Q – torque

$A = \pi \cdot R^2$ – rotor disc area

R – rotor radius

ρ – air density

ω – angular speed of rotor

- Calculation rotor disc loading

$$(4) \quad \Delta p = \frac{T}{A}$$

- Selection of 5-second periods of steady conditions;
- Calculation of mean values and standard deviation values of each included parameter;
- Nondimensionalization of mean values of static pressure (for each pressure tap) to calculate pressure coefficient Cp:

$$(5) \quad Cp = \frac{\bar{p} - p_{atm}}{\Delta p}$$

where:

\bar{p} – mean value of measured pressure

p_{atm} – atmospheric (ambient) pressure;

- Calculation of an equivalent amplitude of oscillation δp , as a standard deviation of pressure related to the rotor disc load:

$$(6) \quad \delta p = \frac{\sigma(p)}{\Delta p}$$

3. RESULTS

3.1. Impact of height above heliport on Cp

First phase of tests included three different values of height above simulated heliport: 0.5R, 1.0R and 1.5R (where R is the rotor radius). For each value

of height different values of the collective pitch have been included, from 0 to 10° (excluding values where the thrust was negative). Rotor characteristics obtained for these values, i.e. curves of figure of merit FM versus thrust coefficient C_T , have been presented in Figure 7. The increment of performance in the proximity of the ground (the ground effect), is clearly visible.

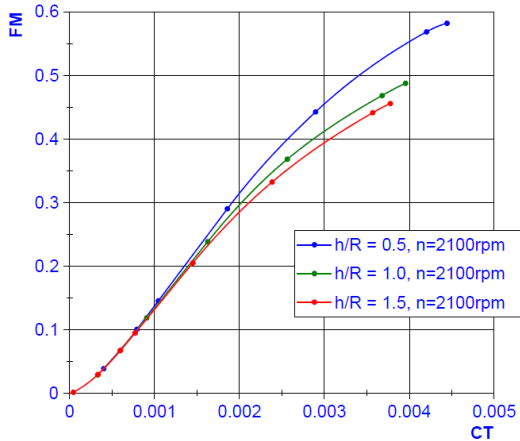


Figure 7. Rotor characteristics for various heights above simulated heliport

Distribution of pressure coefficient versus radial position and thrust coefficient has been presented in Figure 8, Figure 9 and Figure 10 for height of 0.5R, 1.0R and 1.5R respectively. The distributions show clearly that the pressure coefficient achieves its maximum when the height is low: for the height of 0.5R the C_p coefficient achieves value of 0.87. For the height of 1.0R and 1.5R the maximum C_p is 0.70 and 0.58, respectively. The position of the highest pressure coefficient varies from 0.75R to 1.1R approximately; increasing the height shifts the point of maximum pressure towards the blade tip. Obviously, the pressure coefficient increases as the thrust coefficient increases, however this increment is visible at most for radial position from approximately 0.3R to 1.1R.

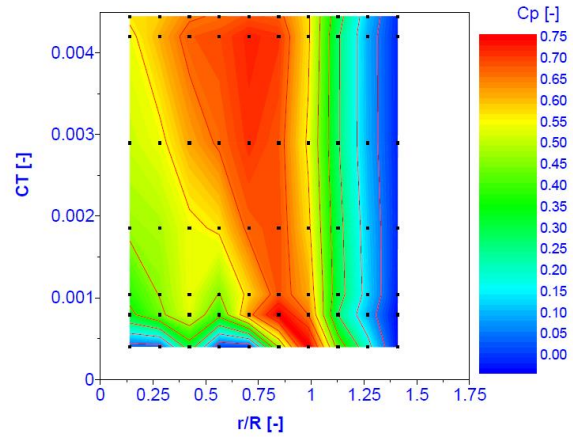


Figure 8. Mean pressure acting on the simulated heliport for the height of 0.5R

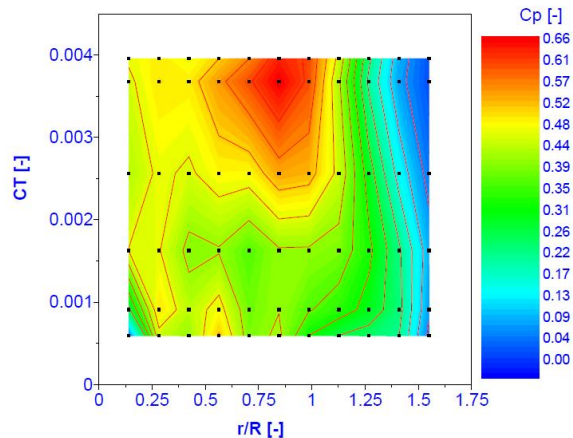


Figure 9. Mean pressure acting on the simulated heliport for the height of 1.0R

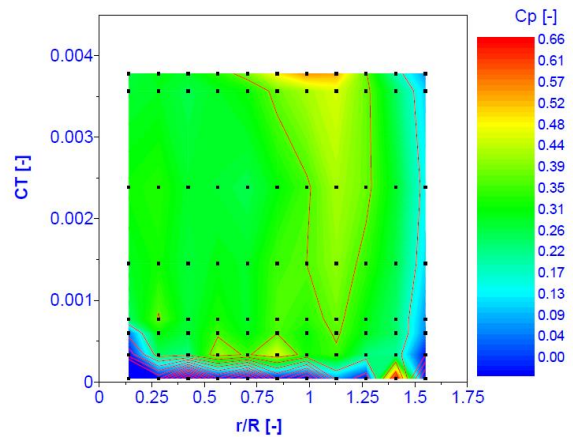


Figure 10. Mean pressure acting on the simulated heliport for the height of 1.5R

3.2. Impact of height above heliport on δp

Similar distributions of equivalent amplitude of pressure oscillation has been presented in Figure 11, Figure 12 and Figure 13 for the height of 0.5R, 1.0R and 1.5R respectively. The highest amplitudes have been captured for minimum values of thrust coefficient, and thus for the minimum values of rotor disc loading. Values of the equivalent amplitude achieves 0.5 for the height of 0.5R. For greater height the maximum captured amplitude decreases for roughly 0.3, however it seems to be dependent from the minimum included thrust coefficient, as one can deduce from a density of isolines in this area.

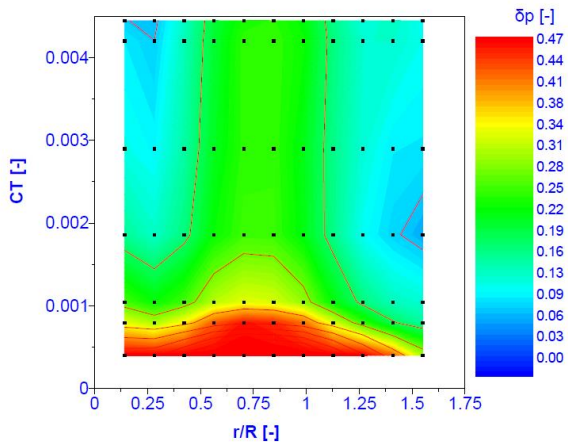


Figure 11. Equivalent amplitude of pressure oscillation for the height of 0.5R

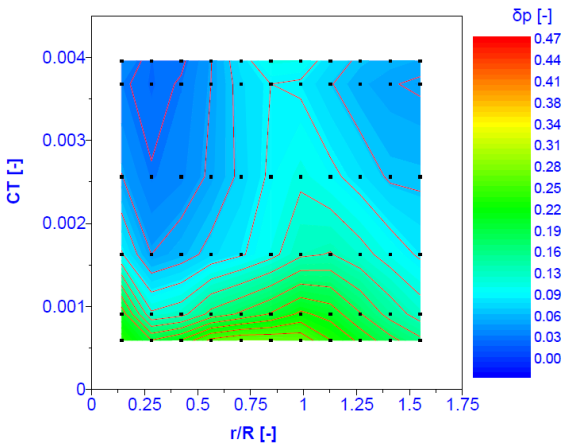


Figure 12. Equivalent amplitude of pressure oscillation for the height of 1.0R

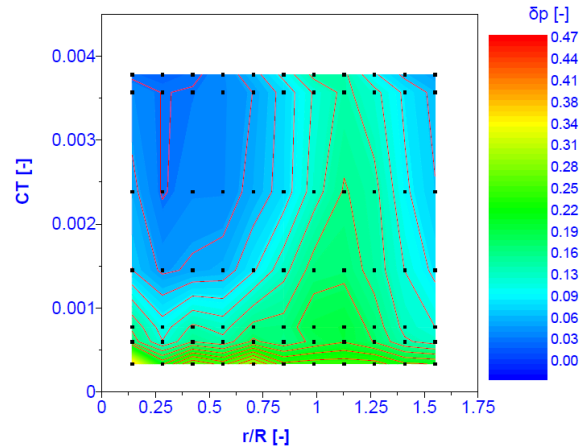


Figure 13. Equivalent amplitude of pressure oscillation for the height of 1.5R

It must be noted that for moderate values of thrust coefficient C_T (over 0.001), one can observe a qualitative change of distributions of equivalent amplitude of oscillation. For the height of 0.5R and 1.0R, maximum oscillation amplitude may be observed for radial location of about 0.8R. Meanwhile, for the height of 1.5R one can observe that the increased oscillation amplitude appears nearby the rotor tips, for the radial location of about 1.1R. However, it should be underlined that for all included heights maximum amplitude of oscillation was captured in proximity of maximum mean pressure.

A difference in δp distributions has been presented more clearly in Figure 14, which contains a comparison of radial distributions of equivalent amplitude of oscillation, plotted for the same value of collective pitch (9°) and thus, for the same value of thrust coefficient OGE (out of ground effect).

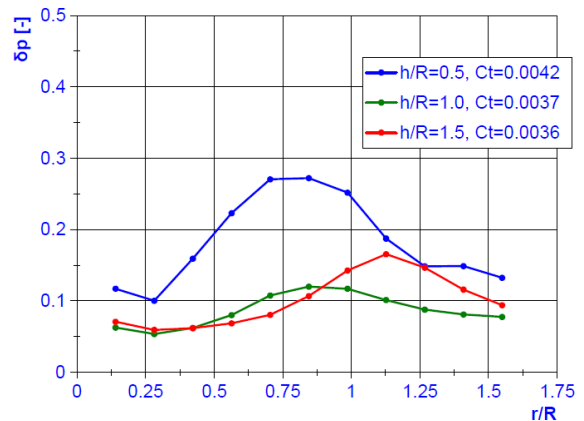


Figure 14. Equivalent amplitude of pressure oscillation for different values of height and for collective pitch of 9° ($C_{T\ OGE}$ approximately 0.0035)

4. VALIDATION OF METHOD

4.1. Reference test stand

To validation the results, distributions of mean pressure and pressure oscillations amplitude obtained for the full-scale rotor has been utilized. The full-scale rotor was a 2-bladed teetering rotor with its diameter of roughly 8 m, placed on the height of 1 radius above the ground. It was mounted on the test stand presented in Figure 15. The pressure underneath the rotor was measured by 5 pressure scanners, placed slightly above the ground (on the height of 15% of radius) to avoid dust. This phase of tests has been described more widely in [15].

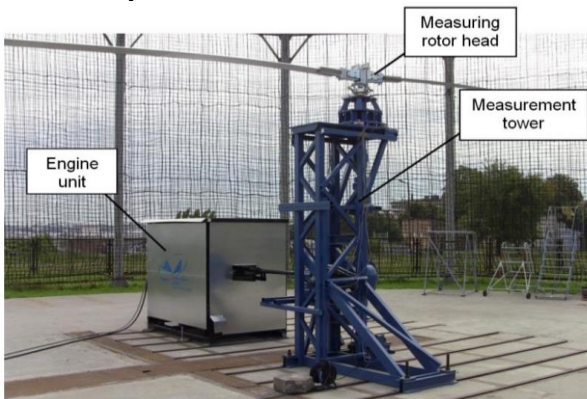


Figure 15. The full-scale rotor on its test stand

The comparison of mean pressure distributions for thrust coefficient of 0.0037 has been presented in Figure 16. Similar comparison of pressure oscillation amplitude has been presented in Figure 17.

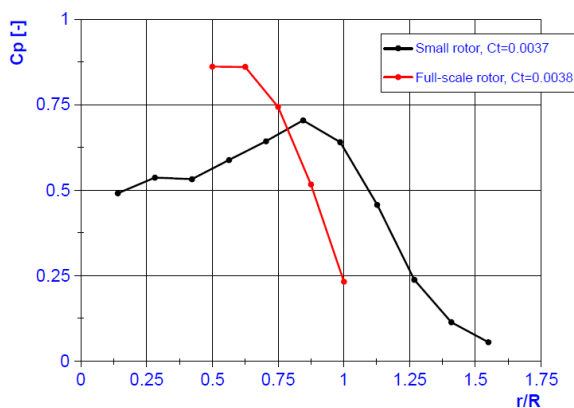


Figure 16. Distribution of mean pressure for investigated rotor and the reference one

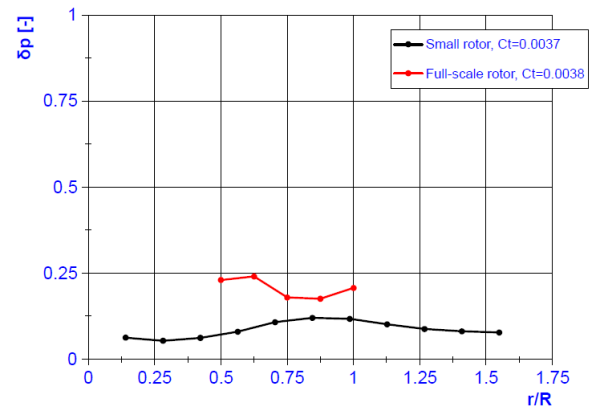


Figure 17. Distribution of pressure oscillation amplitude for investigated rotor and the reference one

As it has been presented, the agreement of mean pressure distribution for both cases is relatively good, taking into account that the measurements for the full-scale rotor have been performed not on the ground level, but slightly above it. This fact explains a shift of maximum pressure location. The distribution of equivalent amplitude of oscillation indicates its maximum in proximity of maximum mean pressure for both cases, however for the full-scale rotor one can observe an increment of oscillation amplitude in outer measurement point. It may be caused by the fact that the test stand was placed in the free air and covered by a security net. This difference may also be the reason of significantly higher amplitude of oscillation obtained for the full-scale rotor.

5. CONCLUSIONS

Presented investigation was aimed on obtaining the amplitude of oscillation of pressure acting on the heliport surface due to the helicopter's slipstream. To estimate this amplitude, the standard deviation of the pressure (calculated for 5-second periods of steady conditions) has been obtained, based on static pressure measurements in pressure taps located on the surface of simulated heliport, underneath the remotely controlled helicopter with rotor diameter of 0.7 m. Results show that the maximum oscillation amplitude is captured in the proximity of maximum mean values of the pressure, which in line strongly depends on the height above the heliport: for the height of 1 radius or lower this area lies roughly in 80% of radius, and for higher values of height the pressure peak shifts outside the rotor, for the radial location of approximately 1.1R for the height of 1.5R. The equivalent amplitude of oscillation (nondimensionalized using rotor disc load) achieves 0.5 for the height of 0.5R and

thrust coefficient of 0.0005. For higher values of height and thrust coefficient the maximum value is approximately equal to 0.2.

The achieved results have been validated using a 8-meter diameter rotor. The agreement of both results is good and differences between them may be explained by differences in test conditions.

6. REFERENCES

- [1] "5 killed as copter on Pan Am Building throws rotor blade." (1977). *The New York Times*, New York.
- [2] Bhagwat, M. J., and Leishman, J. G. (2000). "Stability Analysis of Helicopter Rotor Wakes in Axial Flight." *Journal of the American Helicopter Society*, 45(3), 165–178.
- [3] Corn, J. J., and Horrigan, B. (1984). *Yesterday's tomorrows: past visions of the American future*. Johns Hopkins University Press, Baltimore.
- [4] Dziubiński, A. (2016). "CFD analysis of rotor wake influence on rooftop helipad operations safety." *Transactions of the Institute of Aviation*, 242(1), 7–22.
- [5] Dziubiński, A. (2016). "CFD analysis of wind direction influence on rooftop helipad operations safety." *Transactions of the Institute of Aviation*, 242(1), 23–35.
- [6] Federal Aviation Administration. (2006). *Advisory Circular AC 150/5390-2C: Helipad Design*. 98.
- [7] Gibertini, G., Grassi, D., Parolini, C., Zagaglia, D., and Zanotti, A. (2015). "Experimental investigation on the aerodynamic interaction between a helicopter and ground obstacles." *Proceedings of the Institution of Mechanical Engineers, Part G: Journal of Aerospace Engineering*, 229(8), 1395–1406.
- [8] Horn, J. F., Keller, J. D., Whitehouse, G. R., and Mckillip, R. M. (2011). *Analysis of Urban Airwake Effects on Helipad Operations At the Chicago Children's Memorial Hospital*.
- [9] Johnson, B., Leishman, J. G., and Sydney, A. (2010). "Investigation of Sediment Entrainment Using Dual-Phase, High-Speed Particle Image Velocimetry." *Journal of the American Helicopter Society*, 55(4), 42003-1-42003-16.
- [10] Łusiak, T., Dziubiński, A., and Szumański, K. (2009). "Interference Between Helicopter and Its Surroundings, Experimental and Numerical Analysis." *Task Quarterly*, 13(4), 379–392.
- [11] Mejsner, M. (2011). "Helipads dangerous for structure of buildings (in Polish: Helipady groźne dla konstrukcji budynków)." *Administrator* 24.
- [12] "Pierwsze lądowisko wyniesione w Polsce." (2011). *Urząd Lotnictwa Cywilnego*, <<http://ulc.gov.pl/pl/publikacje/wiadomosci/1259-pierwsze-ladowisko-wyniesione-w-polsce>>.
- [13] *PN-B-02171 standard. Estimation of impact of vibration on people in buildings (in Polish: Ocena wpływu drgań na ludzi w budynkach)*. (2017m).
- [14] Ramasamy, M., Potsdam, M., and Yamauchi, G. K. (2015). "Measurements to Understand the Flow Mechanisms Contributing to Tandem-Rotor Outwash." *71 American Helicopter Society Forum, Virginia Beach, VA, USA, Virginia Beach, VA*.
- [15] Ruchala, P., Dziubinski, A., Stryczniewicz, W., Wojtas, M., and Szumański, K. (2019). "Experimental Investigation of Rotor Slipstream Oscillations in the Ground Effect." *Vertical Flight Society 75th Annual Forum & Technology Display*, Philadelphia, 1–7.
- [16] Smith, A., Bell, A., and Hackett, D. (2017). "Trade-offs in helipad sitting&design." Rowan Williams Davies & Irwin Inc. (RWDI).
- [17] Visingardi, A., De Gregorio, F., Schwarz, T., Schmid, M., Bakker, R., Voutsinas, S., Gallas, Q., Boisard, R., Gibertini, G., Zagaglia, D., Barakos, G. N., Green, R., Chirico, G., and Giuni, M. (2017). "Forces on Obstacles in Rotor Wake – A GARTEUR Action Group." *43rd European Rotorcraft Forum*, Milan.
- [18] *Wykaz lądowisk wpisanych do ewidencji lądowisk na dzień 7 lutego 2019 r.* (2019). *Urząd Lotnictwa Cywilnego, Polska*.